



# Bioactive peptides laden nano and micro-sized particles enriched ECM inspired dressing for skin regeneration in diabetic wounds



C.K. Nanditha<sup>a,b</sup>, G.S. Vinod Kumar<sup>a,\*</sup>

<sup>a</sup> Nano Drug Delivery Systems (NDDS), Bio-Innovation Center (BIC), Rajiv Gandhi Centre for Biotechnology, Thycaud P.O., Thiruvananthapuram, Kerala, 695014, India

<sup>b</sup> Research Centre, University of Kerala, Thiruvananthapuram, Kerala, India

## ARTICLE INFO

### Keywords:

Diabetic wound healing  
ECM like Wound dressing  
Nanofiber functionalization antimicrobial peptide  
Wound healing peptide  
Chronic wound dressing

## ABSTRACT

Hard to heal wounds such as diabetic wounds is one of the major problems in the healthcare sector. Delayed healing and shortfall of functional restoration at the wound site require upgraded wound management aids. In this study, we report that a nanofibrous mat enriched with bioactive peptides laden nano and microparticles achieve the requirements as an effective diabetic wound dressing. By means of electrospinning method, we fabricated Poly (lactic-co-glycolic acid)/Collagen nano-scale mat and surface functionalised with wound healing peptides, laden Chitosan nano and micro-sized particles, creating an Extracellular Matrix (ECM) -like structure with biomimetic features. The developed dressing displayed good cytocompatibility with Keratinocyte and fibroblast cells and enhanced their *in-vitro* cell proliferation and migration. Experiments in the streptozotocin-induced diabetic mice model showed that bioactive peptides released from Chitosan particles shorten the inflammatory stage and promote neovascularisation. The supporting nanoscale matrix promotes increased collagen deposition in the wound beds, thereby hastening the complete healing process by substantial tissue re-generation and functional restoration. The results evince that the nano/microparticles enriched nano-scale mat show potential as an effective wound repair dressing for diabetic wounds.

## 1. Introduction

The wound healing process proceeds through overlapping phases namely, hemostasis, inflammation, proliferation and remodelling stages [1]. But this routine healing is delayed in chronic wound conditions, a major example being diabetic wounds [2]. Prolonged inflammation stage, increased bacterial load and destruction of the extracellular matrix (ECM) at the wound site are some of the reasons for the delay in healing [3–6]. Traditional dressings do not cater to all the needs for chronic wound management, thereby requiring the need for bioactive functionalised dressings efficient to manage the specific needs of wound environment and healing process.

The structural complexity of the extracellular matrix (ECM) can be mimicked by biomaterial-based nanofibrous mats [7,8]. Nanoscale fibers provide a greater surface area and micro-environment for cell proliferation and attachment [9,10]. The high porosity of the nanoscale fiber mats enables high gas permeation and it prevents tissue degeneration [11,12]. The efficiency of electrospun nano-scale fibers can be modulated based on the selection of fiber materials and through surface modification of the nanofibers with bioactive molecules [13,14]. Various bioactive

peptides with therapeutic efficiency in treating chronic wound conditions have been reported. These bioactive peptides range from antimicrobial peptides, which protect against microbial attacks in the wound bed to immuno-modulating and wound healing peptides [15–17]. The bioactive functionalities of such peptides delivered to the wound area through ECM-like nanoscale fibers can ensure the skin regeneration.

In this study, we described an advanced ECM-like matrix biomaterial wound dressing with incorporated dual bioactive peptides that will enhance healing by regulating cell proliferation, preventing bacterial invasion, and providing a matrix helping in collagen remodelling at the wound bed thereby promoting tissue regeneration. In this system, the nanoscale Poly (lactic-co-glycolic acid) (PLGA) and Collagen blended fibrous mat was prepared by the electrospinning method. PLGA has excellent biocompatibility and biodegradability and in combination with an ECM component like Collagen, makes a suitable biomaterial dressing providing extracellular matrix-like architecture [18,19].

Bioactive functionalization with peptides carrying Chitosan nano and micro-sized particles provides an advantage for healing diabetic wounds. Tylotoin is a 12 amino acid sequence (KCVRQNNKRVCCK) bioactive peptide derived from salamander (*Tylostotriton verrucosus*) skin tissue and

\* Corresponding author.

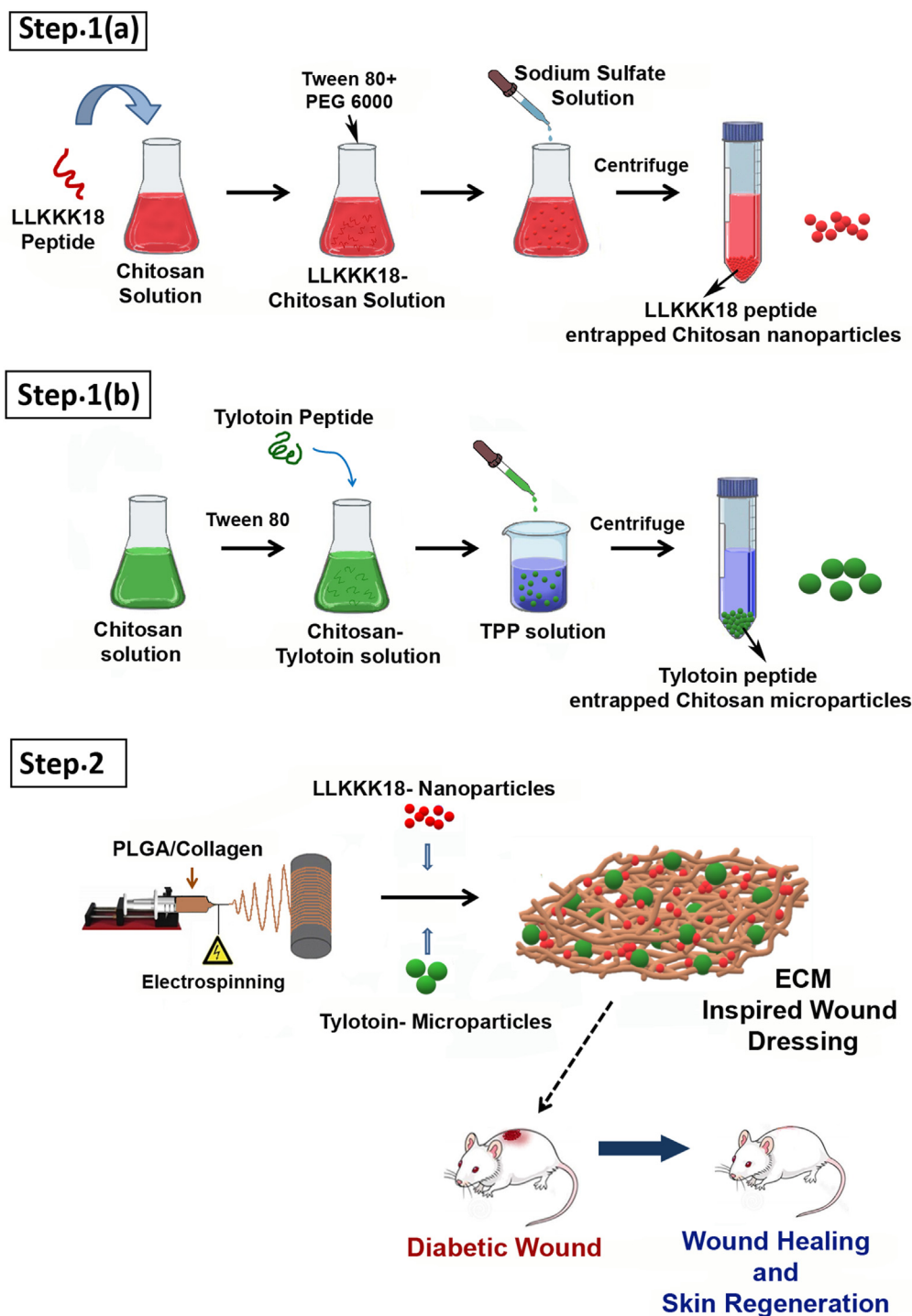
E-mail address: [gsvinod@rgcb.res.in](mailto:gsvinod@rgcb.res.in) (G.S.V. Kumar).

<https://doi.org/10.1016/j.mtbio.2022.100235>

Received 2 February 2022; Received in revised form 2 March 2022; Accepted 5 March 2022

Available online 8 March 2022

2590-0064/© 2022 Published by Elsevier Ltd. This is an open access article under the CC BY-NC-ND license (<http://creativecommons.org/licenses/by-nc-nd/4.0/>).



**Scheme 1.** Schematic illustration of the synthesis of Bioactive Peptides laden nano/micro-sized particles enriched ECM inspired dressing for diabetic wound management. **Step 1(a):** Synthesis of LLKKK18 entrapped Chitosan nanoparticles; **Step 1(b):** Synthesis of Tylostin entrapped Chitosan microparticles, **Step 2:** Synthesis of electrospun PLGA/Collagen nanofibers and conjugation of nano/micro-sized particles to nanofibers to create ECM inspired wound dressing.

it directly enhances the proliferation of keratinocytes, vascular endothelial cells, and fibroblasts and also facilitates the release of more TGF- $\beta$ 1 in dose-dependent manner [20]. LLKKK18 antimicrobial peptide (KLFKRIVKRILKFLRKL) inhibits the growth of *Escherichia coli*, *Pseudomonas aeruginosa*, *Staphylococcus aureus*, and *Candida albicans* [21,22]. In chronic wounds, LLKKK18 is shown to reduce oxidative stress, inflammation and stimulate angiogenesis [23]. In this study, LLKKK18 peptide was entrapped in Chitosan nano-sized particles and Tylostin peptide was entrapped in Chitosan micro-sized particles. The differential release of

LLKKK18 antimicrobial peptide from nano-sized particles and wound healing Tylostin peptide from micro-sized particles during the healing phases would significantly enhance diabetic wound healing by protecting the wound bed from bacterial invasion; and equally inducing cell proliferation, granulation tissue deposition, angiogenesis, collagen deposition, re-epithelialisation and skin regeneration. We analysed the ability of the developed wound dressing in promoting keratinocyte and fibroblast cell survival and migration, leading to faster wound closure. Further, the ability of the developed system to promote diabetic wound

healing in the full-thickness wounds in streptozocin induced mouse model was examined, thereby showing the practical applications of the developed dressing in healing diabetic wounds (Scheme 1).

## 2. Experimental section

### 2.1. Materials

Collagen (from bovine achilles tendon), Chitosan (low molecular weight, Mw. 13000–23000), PLGA (Mw. 24,000–38000, 50:50, acid terminated), 1-Ethyl-3-(3-dimethylaminopropyl) carbodiimide (EDC), N-hydroxysuccinimide (NHS), Tripolyphosphate (TPP), 4-(Hydroxymethyl) phenoxyacetic acid (HMPA) Linker, N-hydroxybenzotriazole (HOBT), O-Benzotriazole-N,N,N',N'-Tertamethyl-Uronium-hexafluorophosphate (HBTU), N,N-Diisopropylethylamine (DIEA), Ninhydrin, Piperidine, Dimethylformamide (DMF), Dichloromethane (DCM), Diethylether, Tri-fluoroacetic acid (TFA), Triisopropylsilane (TIS) and 3-(4,5-dimethylthiazol-2-yl)-2,5-diphenyltetrazolium bromide (MTT) were procured from Sigma, Polyethylene glycol (PEG) (Mw. 6000), DMSO, Trifluoroacetic acid (TFA) and acetone was from MERK and Hexafluoro-2-propanol was from Spectrochem, TentaGel™ resin, F-moc Amino acids from Peptides International, Fetal bovine serum (FBS) was purchased from Hyclone, and live/dead assay kit were from Invitrogen. The cell lines were purchased from National Centre for Cell Science (NCCS), Pune, India.

### 2.2. Preparation of LLKKK18 peptide entrapped chitosan nanoparticle

Chitosan low molecular weight (0.3% w/v) was dissolved in aqueous acetic acid (2% v/v) and added with 100 µg/ml of LLKKK18 peptide (synthesized by solid-phase peptide synthesis using the standard Fmoc-Strategy [24,25]) and kept for stirring for 30min. Tween 80 (4 wt %), PEG 6000 (15 wt %) was added to the solution as a stabilizer. Sodium sulfate solution (20 wt %) was added dropwise to the chitosan solution under simultaneous stirring at 420 rpm and ultrasonicated. Chitosan nanoparticles were separated from the supernatant by centrifugation at 8000 rpm and redispersed in water and lyophilized [26]. The size of the particles was checked by performing DLS–Dynamic Light Scattering Test (Beckman Coulter – Delsa Nano C).

### 2.3. Preparation of Tylotoin Peptide entrapped chitosan microparticle

Chitosan low molecular weight (2% w/v) solutions were prepared by dissolving it in 1% acetic acid and Tween 80 (2% v/v) was added into the solution as a surfactant. 100 µg/ml of Tylotoin peptide (synthesized by solid-phase peptide synthesis using the standard Fmoc-Strategy [24,25]) was added and kept for stirring for 30min. The above solution was added into TPP solution (10%) dropwise and kept for stirring. Chitosan microparticles were separated from the supernatant by centrifugation at 10,000 rpm and redispersed in water and lyophilized [27]. The size of the particles was checked by performing DLS – Dynamic Light Scattering Test (Beckman Coulter–Delsa Nano C).

### 2.4. Bioactive peptides release from nano and micro-scale particles

The bioactive peptides release study from Tylotoin entrapped Chitosan microparticle and LLKKK18 entrapped Chitosan nanoparticle was conducted separately using Micro BCA (Bicinchoninic acid) Protein Assay Kit from Thermo Fisher Scientific. The nano and micro-sized particles weighing 10 mg each were loaded into 3500 Da dialysis membranes and placed in the 50 ml of PBS solution (pH 7.4) in an orbital shaker at 37 °C. 100 µl of PBS solution was collected from both samples at predetermined time points. The standard curve of both Tylotoin and LLKKK18 peptide were plotted and the amount of peptide released at the different time points was quantified by the BCA kit by taking OD (optical density) at 562 nm. The peptide loading efficiency of Tylotoin and LLKKK18 in the micro and nano-particles was determined by measuring

the concentration of the peptides in washing solutions collected during the nano and micro-particle preparation process.

### 2.5. PLGA-collagen nanoscale fiber mat preparation and characterization

PLGA acid terminated (50:50) and collagen was dissolved in Hexafluoroisopropanol (HFIP) solution and blended in the ratio 4:1. The solutions were electrospun at a flow rate of 0.2 ml/h, at a voltage of +20 kV and the tip to collector distance of 15 cm. The synthesized nanofiber mat was characterized by FTIR (Fourier Transform Infrared) spectroscopy (PerkinElmer Spectrum 65 FT-IR Spectrometer by ATR method) and DSC – Differential Scanning calorimeter (PerkinElmer 6000 Differential Scanning Calorimeter).

For the preparation of bioactive peptides carrying chitosan nano and micro-scale particle loaded electrospun mats, the nano/microparticle was dispersed in distilled water, sonicated and added to the EDC/NHS activated PLGA-collagen electrospun mat and kept overnight. The electrospun mats were thoroughly washed several times with distilled water, dried and stored at (–20 °C) for further use. The morphology of the nanofiber mats dressing was characterized by FE-SEM (Field Emission- Scanning Electron Microscopy) (FEI Nova NanoSEM 450).

### 2.6. In-vitro degradation ability

The *in-vitro* degradation of Bioactive Peptides laden nano/micro-sized particles enriched PLGA/Collagen nanofiber dressing was investigated by using PBS, pH 7.4. The test samples with pre-weighed and incubated at 37 °C in 0.1 M PBS (pH 7.4) for 22 days. The samples were then taken out from PBS, washed, freeze-dried, and weighed at different time intervals. The degradation ratio (%) of the test samples ( $D_s$ ) was calculated as:

$$D_s = (X_0 - X_t) / X_0 \times 100, \text{ where } X_0 \text{ is the original weight of the sample and } X_t \text{ is the weight of the sample after a specific time point.}$$

### 2.7. Cytocompatibility testing of bioactive peptides laden nano and micro-sized particles enriched ECM inspired dressing

The keratinocyte cell line (HaCaT) and mouse fibroblast cell line (L929) was purchased from National Centre for Cell Science (NCCS), Pune. The cells were grown in medium (DMEM supplemented with 10% FBS and 1% antibiotics).

*In vitro* cytotoxicity and viability, testing was conducted using the MTT (3-(4,5-dimethylthiazol-2-yl)-2,5-diphenyltetrazolium bromide) assay and Live/Dead staining experiments. MTT assay was done in HaCaT and L929 cells, seeded in 96 well plate ( $5 \times 10^3$  cells/well) and grown under standard growth conditions for 24 h. Media treated with Control (PBS, pH 7.4), Tylotoin carrying chitosan microparticles (Tylotoin-MP) and LLKKK18 carrying chitosan nanoparticles (LLKKK18-NP) 500 µg/ml each, PLGA/Collagen ECM-like nanofiber mat (NF) and Bioactive peptides carrying nano and micro-sized particles enriched ECM-like nanofiber mat dressing (NF-NP-MP) were added to wells containing cells and incubated for different periods (Days 1,2 and 3). After each time interval, the cells were incubated for 4 h with 10% v/v MTT dissolved in PBS, pH 7.4. After removing media, the formazan crystals formed were dissolved in isopropyl alcohol (IPA). Absorbance was measured at 570 nm using BioradiMark™ Microplate Absorbance Reader. Cell viability % was calculated using the formula: [OD of test sample (Avg.)/OD of control (Avg.)  $\times$  100].

For Live/Dead cell assay, HaCaT and L929 cells ( $1 \times 10^5$  cells/well) were grown on a 12-well plate with serum-free medium containing the test samples and were incubated for 72 h. The cells were then stained with calcein AM and ethidium homodimer-1 to distinguish the population of live cells. The cell morphology was visualized using a laser confocal microscope (TCS SP2; Leica Microsystems, Wetzlar, Germany).

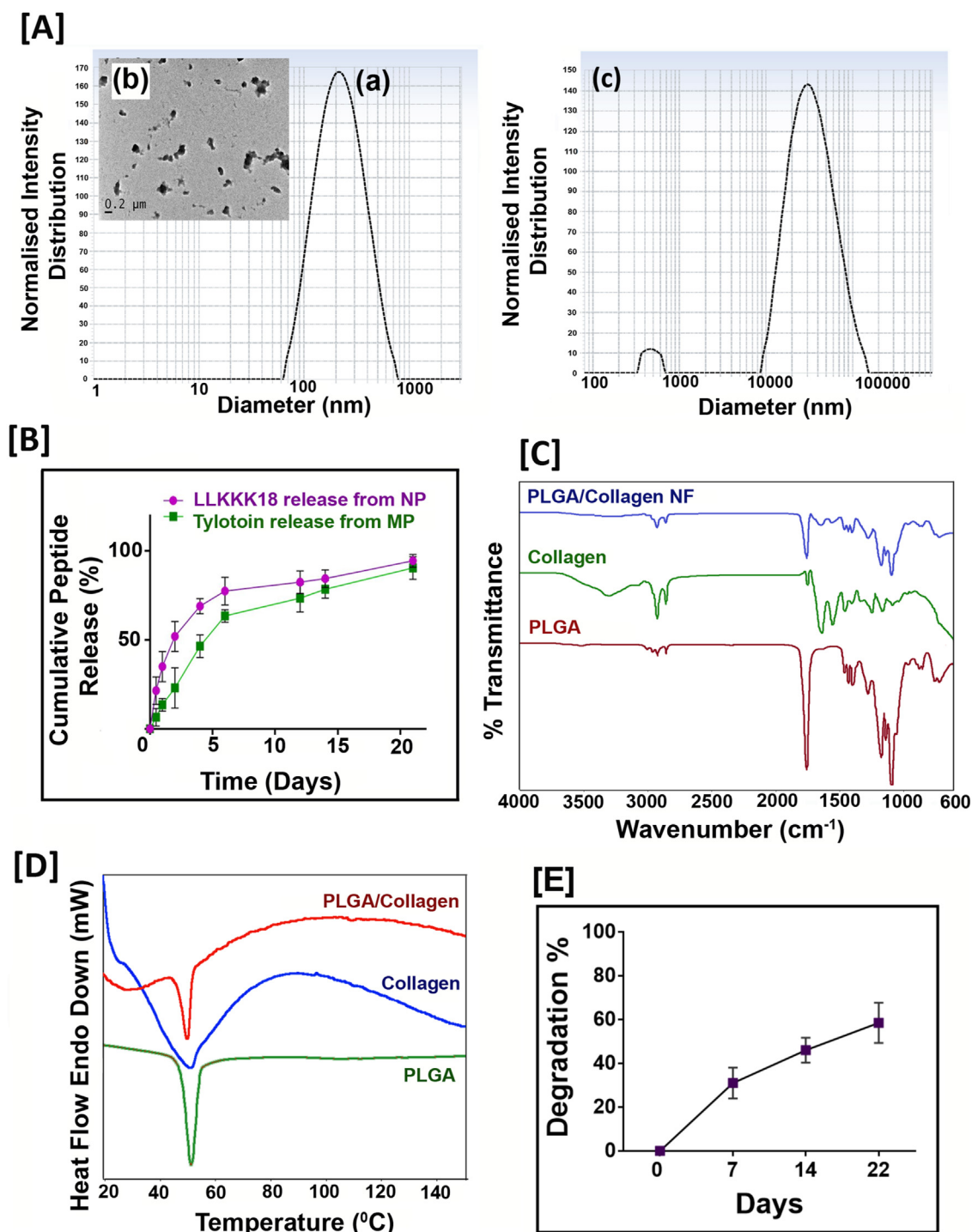
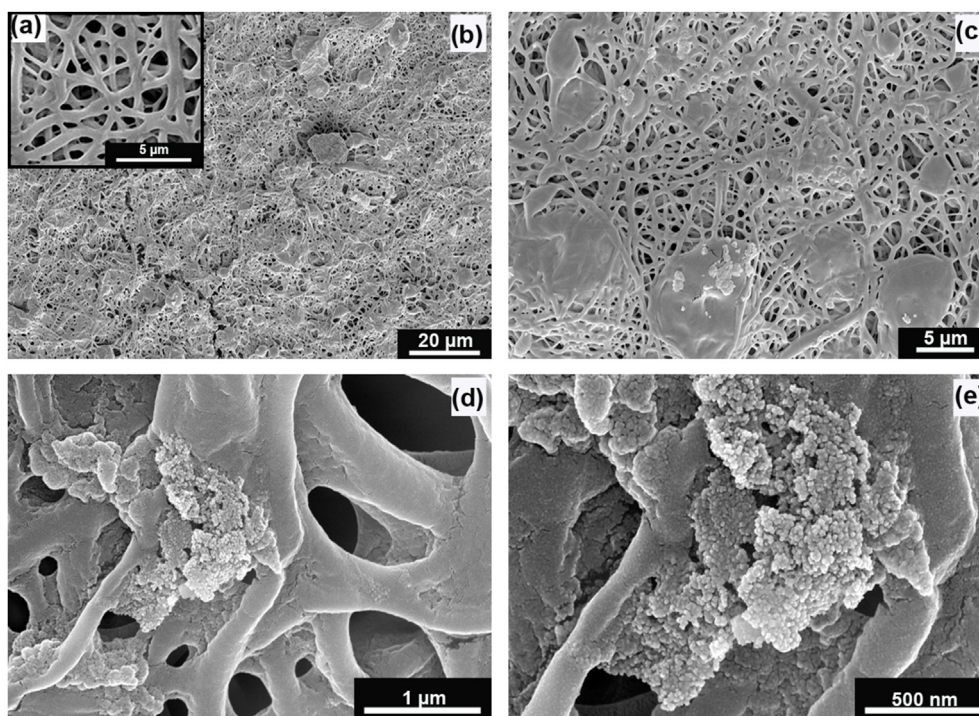


Fig. 1. Characterization [A] DLS (Dynamic Light Scattering) analysis of (a) LLKKK18 peptide entrapped chitosan nanoparticles and (c) Tylotoin Peptide entrapped Chitosan microparticles, (b) TEM (Transmission Electron Microscope) image of LLKKK18 peptide entrapped Chitosan nanoparticles. [B] Peptide release profile from Chitosan nanoparticles and Chitosan microparticles. [C] FT-IR spectrum of PLGA, Collagen and PLGA/Collagen nano-fibers. [D] DSC thermogram of PLGA, Collagen and PLGA/Collagen nano-fibers. [E] *In-vitro* degradation of bioactive peptides laden nano/micro-sized particles enriched PLGA/Collagen nano-fiber mat.

## 2.8. *In-vitro* wound healing assay

The HaCaT and L929 cells were grown in 12 well plates until reaching confluency and were then injured with 2.5  $\mu$ L pipette tip forming a uniform cell-free zone. The wells were washed with PBS to remove cellular debris. Media treated with Control (PBS, pH 7.4), Tylotoin- MP, LLKKK18-NP (500  $\mu$ g/ml each), PLGA/Collagen nanofiber mat (NF). Bioactive peptides carrying nano and micro-sized particles enriched

ECM-like nanofiber mat dressing (NF-NP-MP) were added to the wells and incubated for 24 h (L929) and 48 h (HaCaT). The cell culture wells were imaged at 0, 12, 24, and 48 h time points and the wound closure (diameter in  $\mu$ m) between wound edges was calculated with a computer-assisted analysis system (Olympus CellSens). The wound closure percentage was calculated using the formula: *In-vitro* wound closure % =  $(\text{Pre-migration})_{\text{diameter}} - (\text{Migration})_{\text{diameter}} / (\text{Pre-migration})_{\text{diameter}} \times 100$  [18].



**Fig. 2.** SEM images of (a) PLGA/Collagen nano-fibers, (b) Bioactive peptides laden nano/micro-sized particles enriched PLGA/Collagen nano-fiber mat (ECM inspired wound dressing: 3000 $\times$  magnification), (c) ECM inspired wound dressing showing micro-particles at 10,000 $\times$  magnification, (d) ECM inspired wound dressing showing nano-particles at 100,000 $\times$  magnification, (e) Chitosan nano-particles at 200,000 $\times$  magnification.

### 2.9. Animal studies

All experimental procedures involving animals were approved by the Institutional Animal Ethics committee at Rajiv Gandhi Centre for Biotechnology (IAEC/799/GSV/2020). Swiss albino mice (males) of 4–6 weeks of age, weighing 25–30 g were injected with streptozotocin (STZ-single dose of 180 mg/kg) as per standardized protocol [28,29]. After 4 days from the injection, whole-blood glucose was determined using a blood glucose monitoring system (Accu-Chek) and mice with blood glucose levels more than 300 mg/dL were considered diabetic. Animals were then anesthetized using Isoflurane inhalation anesthesia and the dorsal surface of each animal was shaved and sterilized with 70% ethanol. A full-thickness excisional skin wound of 8 mm-diameter was created using a sterile biopsy punch [30]. After surgery, the mice were randomly divided into wounds treated with Control (PBS, pH 7.4), LLKKK18-NP (LLKKK18 peptide entrapped chitosan nanoparticles), Tylotoin-MP (Tylotoin peptide entrapped chitosan microparticles), NF (PLGA/Collagen electrospun nano-scale fiber mat) and NF-NP- MP (Bioactive peptides carrying nano and micro-sized particles enriched ECM-like nanofiber mat dressing). The appropriate treatment materials were applied to the wound site based on each group. After surgery, the wounds were sutured along the wound boundary with silicone sheet to avoid skin contraction. The wound closure after treatment application was monitored on 0, 7, 14 and 21 days. Wound closure rate (%) was calculated using the formula: Wound healing rate =  $[\text{Area}_{(0 \text{ day})} - \text{Area}_{(n \text{ day})}] / (\text{Area}_{(0 \text{ day})}) \times 100\%$  ('n' represents 7, 14 and 21 days after wound creation). The animals were sacrificed at 7, 14 and 21 days for the histological analysis and the tissue was sectioned (5- $\mu\text{m}$ ) after paraffin embedding. The samples were analysed by hematoxylin and eosin (H&E) staining and Masson's trichrome staining (Trichrome Stain Kit, Abcam). The Quantitative analysis was performed using Image-J software.

### 2.10. Statistics

The experiments performed were done in triplicates and the data

were analysed using GraphPad Prism™ software (version 6). Statistical analysis was done by means of a two-way analysis of variance (ANOVA, non-parametric analysis). Data are shown as the mean  $\pm$  standard deviation (SD),  $n = 3$ , with significance accepted when  $p < 0.05$ .

## 3. Results and discussion

### 3.1. Characterization and morphology of the bioactive peptides laden nano and micro-sized particles enriched ECM inspired dressing

Functionalizing a wound dressing with therapeutic bioactive agents can help address various chronic wound complications like infections, inflammation, and lack of cell proliferation, thereby promoting efficient wound repair [31,32]. Bioactive agents like peptides, when applied directly to the wound site, can result in enzymatic degradation and poor bioavailability. Regulated and differential delivery of dual bioactive peptides to the wound site using nano and micro-sized particles and an ECM-like matrix can help regenerate functional tissues. Also, surface functionalization after the electrospinning process protects the bioactive agents inside the particles from solvent exposure [13].

Chitosan-based particles are an ideal biomaterial carrier for peptides and controlled release [33]. We synthesized two different sized chitosan particles for the differential release of two different bioactive peptides: (a) LLKKK18 peptide entrapped chitosan nanoparticles and (b) Tylotoin Peptide entrapped Chitosan microparticles were synthesized. The mean particle size of the nanoparticles and microparticles was determined by Dynamic Light Scattering (DLS) (Fig. 1 (A) a, c) and the hydrodynamic size of LLKKK18 peptide entrapped chitosan nanoparticle was found to be  $180 \pm 6.2$  nm. TEM (Transmission Electron Microscope) image (Fig. 1(A) b) shows slightly aggregated nanoparticles with less than 200 nm size. The size of Tylotoin entrapped Chitosan microparticles was found to be  $10 \pm 3.7$   $\mu\text{m}$ . The encapsulation efficiency of LLKKK 18 peptide in chitosan nanoparticle was determined to be 84.93% and that of Tylotoin in Chitosan micro-particles was found to be 78.40%. Using different methods for Chitosan nano and micro-sized particles preparation, we

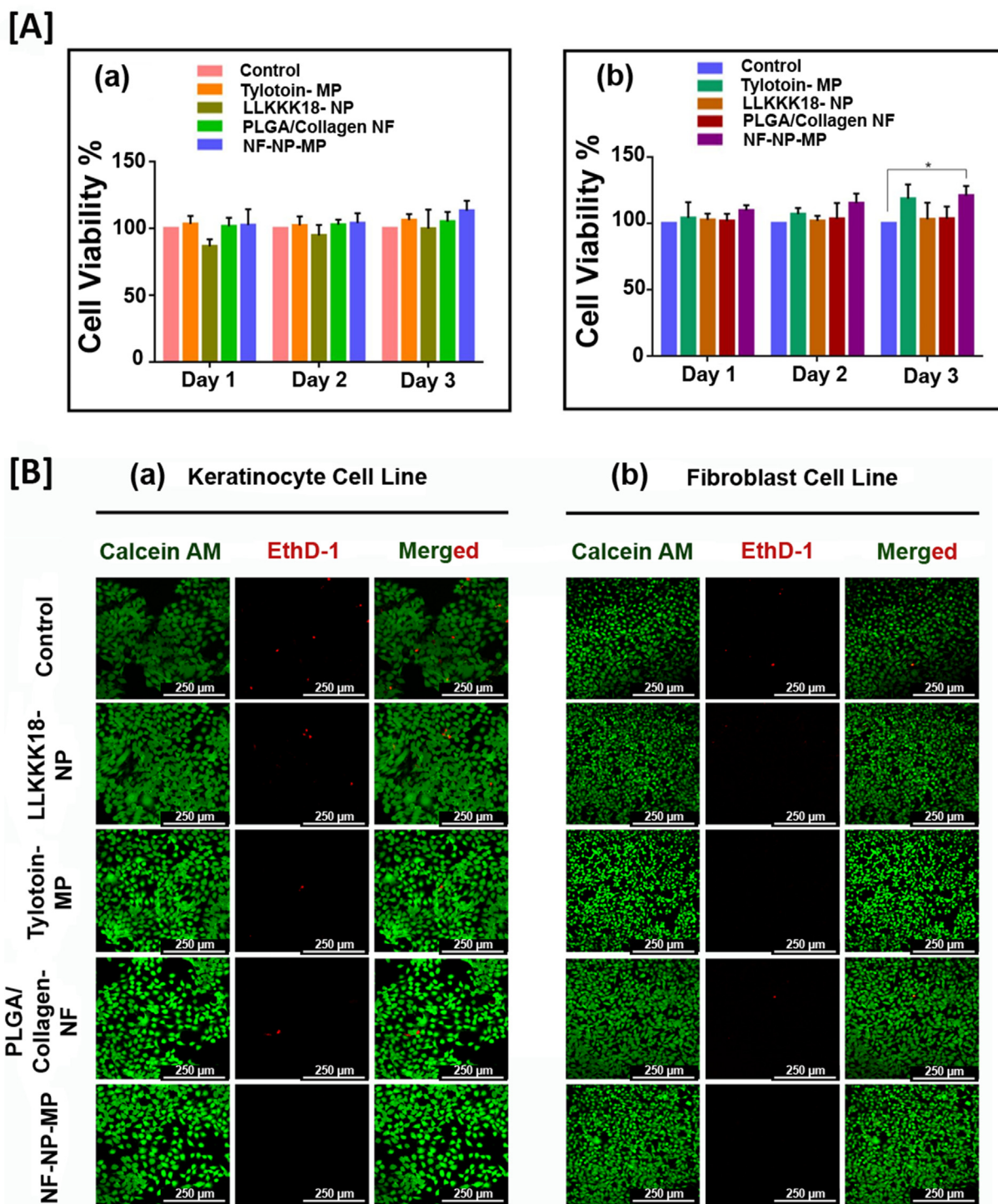


**Fig. 3.** *In-vitro* cyto-compatibility of the bioactive peptide releasing ECM like nano-fiber mats [A] MTT assay of cell proliferation in (a) HaCaT cell line, (b) L929 cell line. Results expressed as mean  $\pm$  SD ( $n = 3$ ,  $*P < 0.05$ ). [B] Live/dead Cell Survival Assay in (a) HaCaT cell line, (b) L929 cell line. Scale bar: 250  $\mu$ m. **Treatments:** Control (0.1 M PBS, pH 7.4), LLKKK18 - Chitosan NP (LLKKK18 peptide entrapped Chitosan nanoparticles), Tylotoin - Chitosan MP (Tylotoin peptide entrapped Chitosan microparticles), PLGA/Collagen-NF (PLGA/Collagen nanofibers), NF-NP-MP (Bioactive peptides laden nano/micro-sized particles enriched PLGA/Collagen nano-fiber mat).

modulate the release profile of the two entrapped bioactive peptides. The peptides from particles showed a continuous release pattern for over three weeks after a moderate burst release. By the end of 21 days, LLKKK18 peptide showed  $\sim 94\%$  release from Chitosan nanoparticles and Tylotoin peptide showed  $\sim 90\%$  release from Chitosan microparticles. It was observed that LLKKK18 peptide was released faster during the first

two weeks of the study when compared to Tylotoin peptide (Fig. 1(B)). This can help in faster antimicrobial action in infected wounds and the comparatively slower and sustained release of Tylotoin peptide can assist in better healing throughout the healing phases.

The ECM-like nanoscale fibers synthesized by electrospinning produce highly porous fibrous mats, aiding in oxygen permeation. The FT-IR

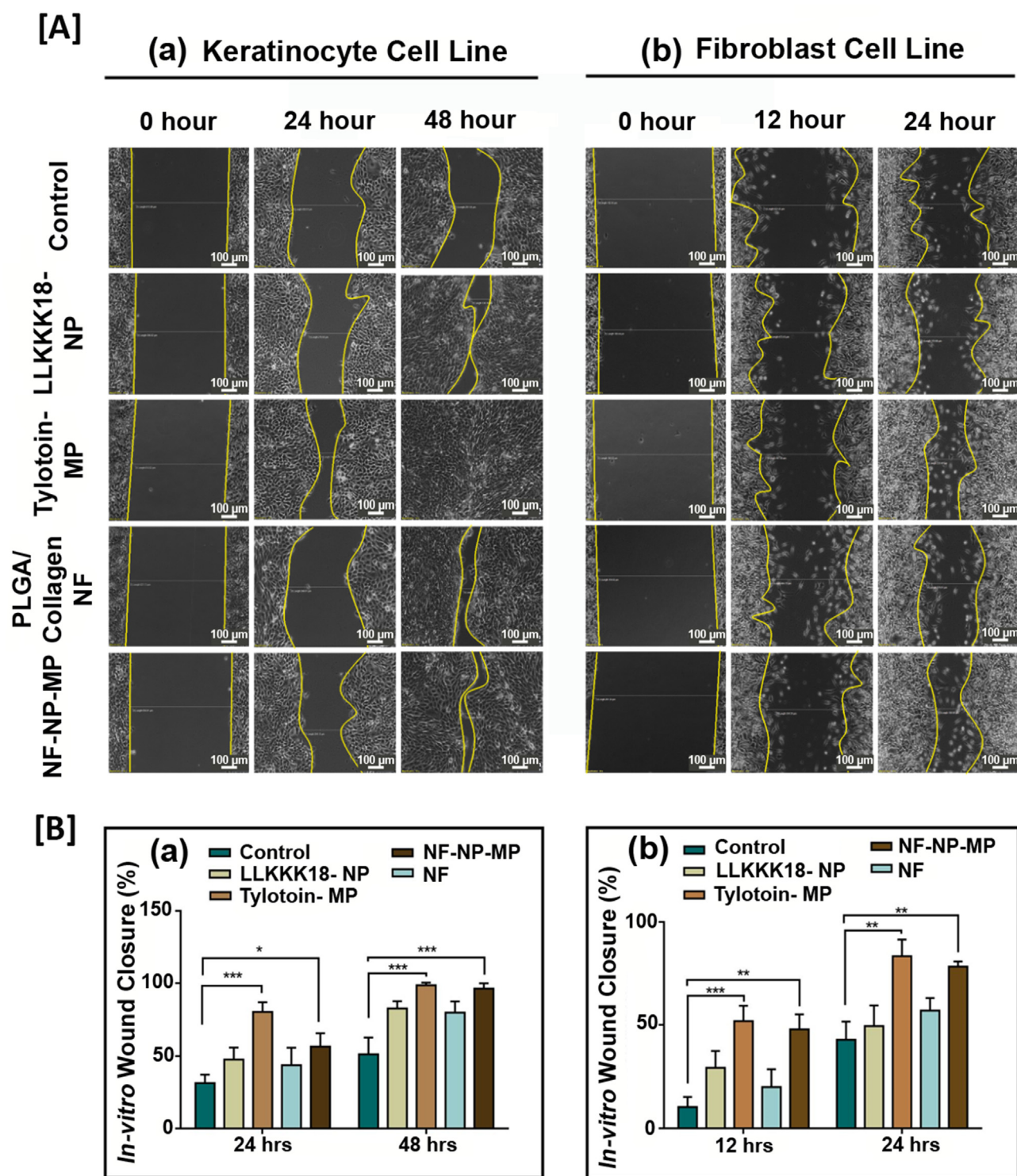
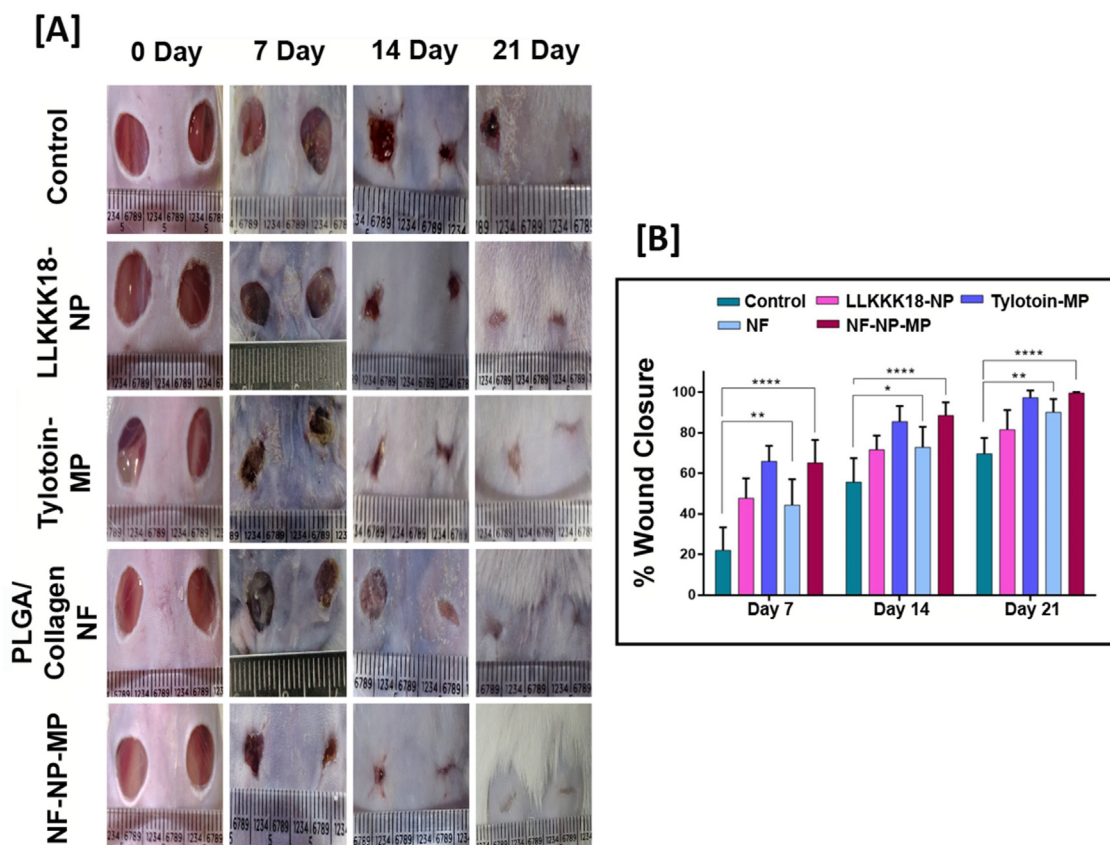


Fig. 4. [A] *In-vitro* wound healing assay images of (a) HaCaT cells obtained at 0, 24 and 48 h after wound creation, (b) L929 cells obtained at 0, 12 and 24 h. Scale bar: 100  $\mu\text{m}$ . [B] Percentage wound closure graph of (a) HaCaT cells and (b) L929 cells. Results expressed as mean  $\pm$  SD ( $n = 3$ ,  $^*P < 0.05$ ). Treatments: Control (0.1 M PBS, pH 7.4), LLKKK18 – Chitosan NP (LLKKK18 peptide entrapped Chitosan nanoparticles), Tylotoin – Chitosan MP (Tylotoin peptide entrapped Chitosan micro-particles), PLGA/Collagen-NF (PLGA/Collagen nanofibers), NF-NP-MP (Bioactive peptides laden nano/micro-sized particles enriched PLGA/Collagen nano-fiber mat).

spectroscopy (Fig. 1(C)) analysis of blended nanofiber shows the characteristic peaks of both PLGA and Collagen. PLGA shows aliphatic C–H stretching peaks at  $3000\text{--}2850\text{ cm}^{-1}$ , carbonyl C=O stretching at  $1850\text{--}1650\text{ cm}^{-1}$ , and ester C–O asymmetric stretching at  $1300\text{--}1000\text{ cm}^{-1}$ . Collagen shows characteristic absorption peaks at  $1650\text{ cm}^{-1}$  amide I, amide II at  $1560\text{ cm}^{-1}$ , and amide III vibration at  $1245\text{ cm}^{-1}$

[19]. The DSC thermogram of each of the individual components PLGA and Collagen and the synthesized nanofiber mat was analysed. An endotherm peak was observed at approximately  $54$  and  $50\text{ }^\circ\text{C}$  for the PLGA and Collagen, respectively. This can be due to the glass transition temperature of PLGA and Collagen. The PLGA/Collagen blended nanofiber mat showed a glass transition temperature peak at  $48\text{--}50\text{ }^\circ\text{C}$ ,



**Fig. 5.** Diabetic wound healing ability of bioactive peptides laden nano/micro-sized particles enriched ECM inspired dressing in streptozocin induced diabetic mice. **[A]** Representative wound healing images of treatment groups tested on day 0, 7, 14 and 21 days. **[B]** Percentage of wound contraction tested on day 7, 14 and 21 days. Results expressed as mean  $\pm$  SD ( $n = 3$ ,  $*P < 0.05$ ). **Treatments:** Control (0.1 M PBS, pH 7.4), LLKKK18 – Chitosan NP (LLKKK18 peptide entrapped Chitosan nanoparticles), Tylotoin – Chitosan MP (Tylotoin peptide entrapped Chitosan microparticles), PLGA/Collagen-NF (PLGA/Collagen nanofibers), NF-NP-MP (Bioactive peptides laden nano/micro-sized particles enriched PLGA/Collagen nano-fiber mat).

indicating that the thermal properties of the PLGA/Collagen nanofiber mat have not been affected during the electrospinning process (Fig. 1(D)). The *in-vitro* degradation of the Bioactive Peptides laden nano/micro-sized particles enriched PLGA/Collagen nanofiber mat (Fig. 1(E)) showed  $\sim 58\%$  weight loss after 22 days of immersion in PBS, pH 7.4. The faster degradation rate can be due to the usage of PLGA (50:50 ratio of lactic acid: glycolic acid) and hydrophilic nature of collagen used for synthesising PLGA/Collagen nanofibers.

The peptide-loaded nano and micro-sized particles were surface conjugated to the synthesized nanofiber mat by EDC/NHS chemistry. The morphology of the synthesized nanofibers was visualized by Scanning Electron Microscopy (Fig. 2). The nanofiber mat showed a high porosity. The nanofibers are of different sizes ranging from 300 to 600 nm, which can be due to the blend of different polymers used in the fabrication. In the SEM images, we could visualise the distribution of micro and nano-sized particles on the nanofiber mat. Chitosan nanoparticles were found to be aggregated due to their polysaccharide nature. The bioactive peptides loaded nano and micro-sized particles released from ECM-like nanofiber mat mimic the healing signals at the physiological wound environment, thereby promoting healing and acting as suitable diabetic wound management aid.

### 3.2. Cell survival and proliferation ability of bioactive peptides laden nano and micro-sized particles enriched ECM inspired dressing

Proliferation and migration of dermal cells are required for wound healing and skin regeneration [34,35]. A suitable wound dressing would support cell survival, adherence and migration. Fabrication of wound

dressing material like nanofibers using natural and synthetic polymers enhance the fiber characteristics and provides a suitable matrix for healing progression [36]. The *in-vitro* cytocompatibility of the bioactive peptide releasing ECM-like nanofiber mats was evaluated in HaCaT and L929 cell cultures (Fig. 3 (A) a, b). The cells were treated with media incubated with the samples, and were used to study the effect on its viability and proliferation. Tylotoin peptide carrying microparticles (Tylotoin-MP) induced HaCaT and L929 cell viability and proliferation based on its bioactive nature. But when compared to the Control (PBS, pH 7.4), LLKKK18 carrying Chitosan nanoparticle (LLKKK18-NP) showed a slight reduction in viability of both cell lines, possibly due to the high positive charged amino-acid presence providing its antimicrobial nature [37]. But, when in combination, the peptides laden nano/micro-sized particles enriched ECM inspired dressing (NF-NP-MP) enhanced cell viability and proliferation of both keratinocyte (HaCaT) and fibroblast (L929) cells studied for 3 days. The developed ECM-like mat dressing treatment will help ineffective healing as viability and proliferation of dermal cells are essential for granulation tissue formation and healing. Live/Dead cell assay (Fig. 3 (B) a, b) at day 3 of treatments on skin cells were conducted. The results corroborated with that of MTT cell viability assay. The combined release of dual tissue regenerating and anti-microbial peptides from ECM-like nano-fiber mats increased the cell survival of HaCaT and L929 cells in *in-vitro* conditions, thereby indicating its efficiency as a suitable wound dressing.

The therapeutic effect of the bioactive peptides released from nano/micro-sized particles enriched ECM-inspired dressing promotes wound healing through skin cell migration. Keratinocytes (part of the epidermis) and fibroblasts play an important role during wound repair upon injury

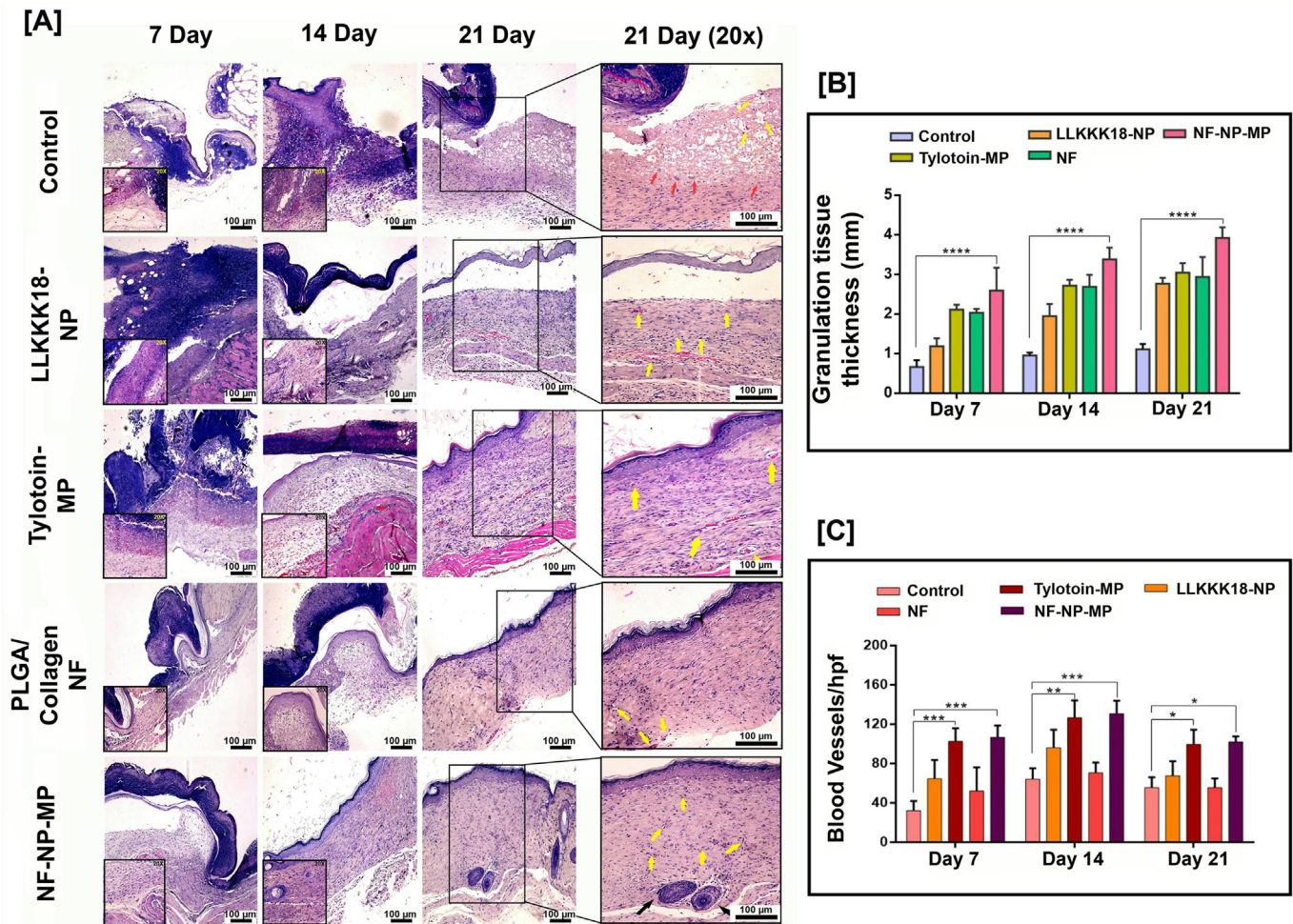


**Fig. 6.** Morphology of regenerated skin upon wound closure. **[A]** Representative H&E staining images of wound biopsy samples at Days 7, 14 and 21. (Arrows: Yellow- Neovascularisation, Red- Inflammatory cells, Black- Glandular Adnexa). Scale bar: 100  $\mu$ m. **[B]** Granulation tissue thickness (in mm) of wound healing after treatment applications. **[C]** Histomorphometrical analysis of angiogenesis. Blood vessel (hpf - High powered field) formation in wound biopsy samples. Results expressed as mean  $\pm$  SD (n = 3, \*P < 0.05). **Treatments:** Control (0.1 M PBS, pH 7.4), LLKKK18 - Chitosan NP (LLKKK18 peptide entrapped Chitosan nanoparticles), Tylotoin - Chitosan MP (Tylotoin peptide entrapped Chitosan microparticles), PLGA/Collagen-NF (PLGA/Collagen nanofibers), NF-NP-MP (Bioactive peptides laden nano/micro-sized particles enriched PLGA/Collagen nano-fiber mat).

through the process of epithelialisation and granulation tissue formation. We analysed the pro-migratory effect of the developed system through an *in-vitro* wound closure assay. To ensure the migration effect, cells were serum-starved for 24 h before creating injury and treatment application. Complete wound closure of HaCaT (by 48 h) (Fig. 4 (A) a, (B) a) was observed on Tylotoin -MP treatment (Tylotoin entrapped microparticles) suggesting its bioactive therapeutic potential when compared to control. Faster L929 cell migration was observed in Tylotoin -MP treatment by 24 h (Fig. 4 (A) b, (B) b). The combination effect of bioactive peptides released from ECM-inspired dressing treatment increased the migration rate of HaCaT (keratinocytes) and L929 (fibroblasts), suggesting its potential in injury repair.

### 3.3. Diabetic wound closure ability of bioactive peptides laden nano/micro-sized particles enriched ECM inspired dressing

The potential of the developed wound dressing was further evaluated *in vivo* on streptozocin-induced full-thickness skin defect diabetic mouse model [28,29]. The bioactive peptides released from ECM-like nanofiber dressing enhanced cell viability, proliferative and migratory effect on keratinocytes and fibroblasts. Earlier reports suggest the therapeutic potential of the bioactive peptides in regulating inflammation, cell

proliferation and antimicrobial action. The present study evaluated the combinatorial effect of the released LLKKK18 antimicrobial peptide and Tylotoin peptide from the ECM-like nanofiber mat dressing in diabetic wound closure. Increased wound closure rate in NF-NP-MP (bioactive peptides laden nano/micro-sized particles enriched ECM inspired dressing) group was observed on days 7, 14 and 21 when compared to other groups (Fig. 5 (A), (B)). Diabetic wounds treated with PLGA/Collagen blended nanoscale fiber (NF) show increased wound closure by 21 days compared to the control (PBS, pH 7.4) group. The Tylotoin-MP and LLKKK18- NP treatment groups showed faster healing than the control and NF groups on day 14 showing, their bioactive therapeutic ability. The combinatorial effect of both bioactive peptides along with the ECM-like matrix of our wound dressing enhances its wound healing potential. Diabetic wounds are characterised by a lack of extracellular matrix by enhanced degradation at the wound environment due to the presence of the high amount of inflammatory cytokines [3–6]. LLKKK18 peptide regulates inflammation at chronic wound site along with combating microbial invasion. The faster release of LLKKK18 and growth factor up-regulating Tylotoin peptide's potential combats this issue. The bioavailability of the peptides to the wound site was enhanced by its gradual and prolonged release from nano and micro-scale Chitosan particles. The PLGA/Collagen ECM-like nanofiber supports to the

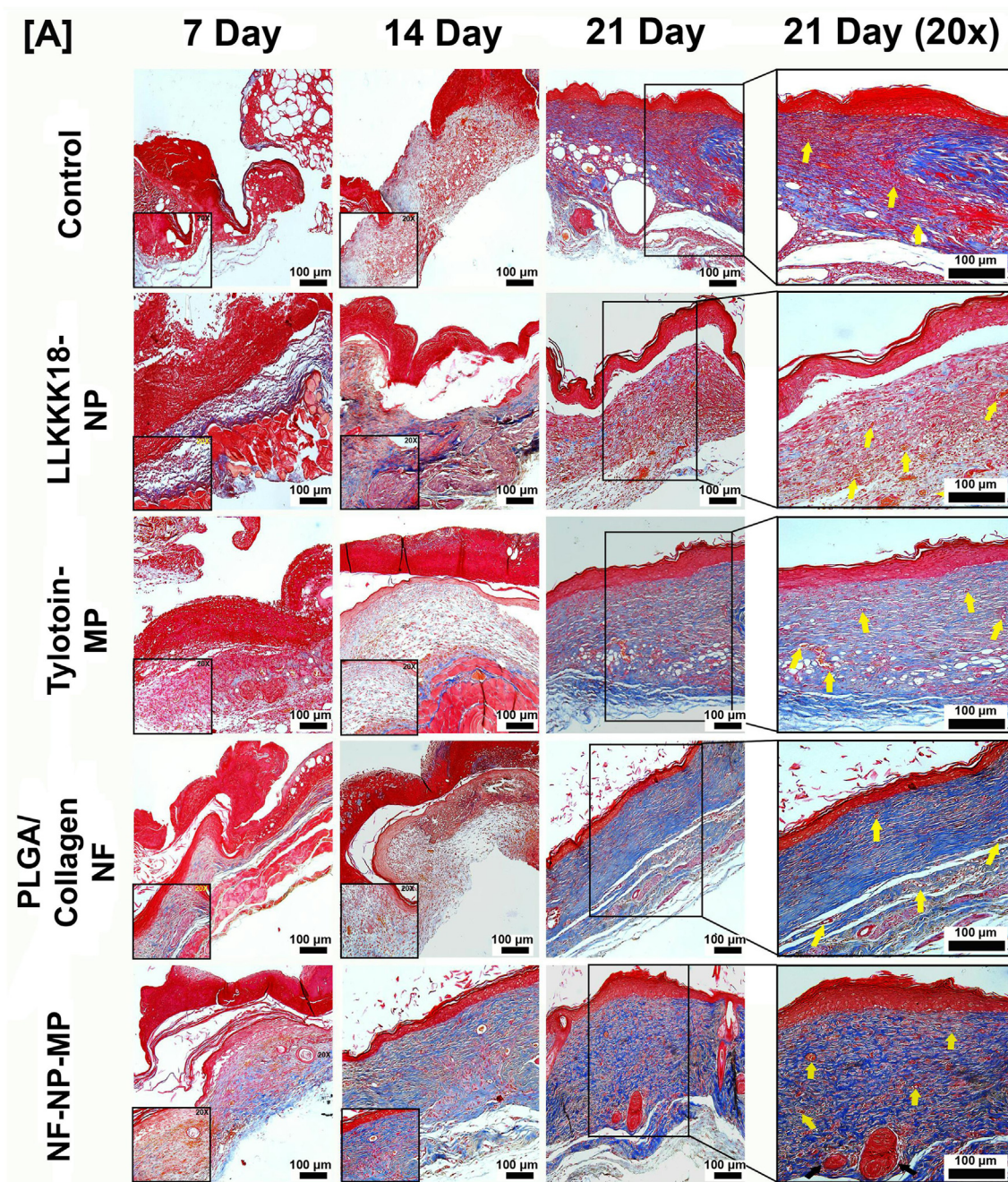


**Fig. 7.** [A] Representative Masson's trichrome staining images of wound biopsy samples at Days 7, 14 and 21. (Arrows: Yellow- Neovascularisation, Black- Glandular Adnexa). Scale bar: 100  $\mu$ m. **Treatments:** Control (0.1 M PBS, pH 7.4), LLKKK18 – Chitosan NP (LLKKK18 peptide entrapped Chitosan nanoparticles), Tylotoin – Chitosan MP (Tylotoin peptide entrapped Chitosan microparticles), PLGA/Collagen-NF (PLGA/Collagen nanofibers), NF-NP-MP (Bioactive peptides laden nano/micro-sized particles enriched PLGA/Collagen nano-fiber mat).

Keratinocyte and fibroblast cell attachment and migration through the wound bed, promoting faster wound closure and healing.

### 3.4. Collagen remodelling, re-epithelialisation and angiogenesis of diabetic wounds by bioactive peptides laden nano/micro-sized particles enriched ECM inspired dressing

The histological assessment of wound tissue after 7, 14 and 21 days of treatment was conducted to understand the healing potential of the developed ECM-inspired dressing. In Hematoxylin and Eosin (H&E) stained sections (Fig. 6 (A)), the NF-NP-MP dressing treatment showed faster re-epithelialisation when compared to the control diabetic group.

Keratinocyte migration ability of the developed dressing promoted its faster re-epithelialisation. By day 14, NF-NP-MP treatment promoted complete re-epithelialisation compared to other treatment groups, and within 21 days, the wound bed showed matured epithelium. Increased granulation tissue formation through fibroblast migration in wounds treated with NF-NP-MP was observed (Fig. 6 (B)). Compared to the control, the wound bed in other treatment groups showed improved healing and a lesser number of inflammatory cells. Neo-vascularisation at the wound bed is essential for skin regeneration and healing in diabetic wounds [38]. Earlier studies have reported the requirement of additional application of angiogenic growth factors such as FGF (fibroblast growth factor) and VEGF (vascular endothelial growth factor) to induce

neovascularisation in diabetic wounds [39,40]. In this study, it was observed that the Tylotoin-MP, LLKKK-18-NP and NF-NP-MP treatments promoted greater neo-vascularisation ability when compared to the Control and NF alone treatment suggesting the growth factor upregulation and blood vessel formation ability of the bioactive peptides applied to the wound bed (Fig. 6 (C)). The wound bed morphology also indicated that upon treatment with NF-NP-MP dressing, the wound has proceeded to the final stages of healing. There is considerable skin regeneration with the presence of hair follicles and sebaceous glands within 21 days.

During wound healing, low levels of collagen deposition occur in the wound bed to close the injury. As the healing progresses, there is increased fibroblast proliferation and collagen deposition and matured bundled collagen is visible in regenerated skin [41,42]. Bioactive Peptides laden nano/micro-sized particles enriched ECM-inspired dressing was analysed by Masson's trichrome staining (Fig. 7) to determine the deposition of collagen. It was observed that in treatment with NF-NP-MP dressings, there was increased collagen deposition by day 14. Application of NF and NF-NP-MP treatment resulted in the formation of matured bundled collagen in the wound bed by 21 days. The presence of Collagen in nanofiber and the fibroblast proliferation and migration ability of the bioactive peptides resulted in faster wound remodelling and closure. Blood vessel formation in treatment groups was also observed. The synergistic effects of the bioactive peptides released from ECM-like nano-scale fiber mat dressings promoted re-epithelialisation, fibroblast proliferation, angiogenesis and collagen deposition resulting in faster diabetic wound healing and Skin maturation.

#### 4. Conclusions

In this study, we developed Bioactive Peptides laden nano/micro-sized particles enriched ECM inspired dressing with diabetic wound healing capability. The developed nanoscale fiber mat provides ECM-like protection and support from further injury when applied to the wound bed. The combinatorial application of antimicrobial and tissue regenerating peptide by differential release from nano and micro-sized particles embedded in nanofiber mat improved skin cell survival, proliferation and migration. When tested for its wound healing efficacy in a streptozotocin-induced diabetic mice model, the developed functionalised dressing showed faster re-epithelialisation, granulation tissue deposition, less inflammation and greater neovascularisation in the wound bed. Elevated Collagen deposition at wound site indicated the faster progression of the wound from inflammatory to remodelling phase, also leading to matured regenerated skin at the wound area. The highly efficient healing potential of the bioactive peptides carrying ECM-like dressing makes it an excellent candidate for therapeutic clinical application in diabetic wounds.

#### Funding

The authors are grateful to the Department of Biotechnology, New Delhi, India for providing the financial assistance for the research work and the University Grants Commission (UGC), New Delhi, India for the Junior Research Fellowship to Nanditha C.K.

#### Author statement

We disclose that this manuscript has not been published previously and is not under consideration of any other journal. All authors agree with the submission of this manuscript to *Materials Today Bio*. We affirm that all *in vivo* work was approved by IACUC and met all institutional, state, and national ethical standards. We declare that there are no conflicts of interest:

#### Declaration of competing interest

The authors declare that they have no known competing financial interests or personal relationships that could have appeared to influence

the work reported in this paper.

#### Acknowledgements

The authors are grateful to Dr. Vishnu Sunil Jaikumar, Veterinarian, RGCB, for his help in conducting Animal experiments, Mr. Anuroop, RGCB for Confocal microscopy imaging, Ms. Viji of RGCB for help with tissue processing and Mr. Basith, Department of Optoelectronics, University of Kerala, Trivandrum for SEM analysis.

#### References

- [1] Y. Yang, X. Zhao, J. Yu, X. Chen, R. Wang, M. Zhang, Q. Zhang, Y. Zhang, S. Wang, Y. Cheng, Bioactive skin-mimicking hydrogel band-aids for diabetic wound healing and infectious skin incision treatment, *Bioact. Mater.* 6 (11) (2021) 3962–3975, <https://doi.org/10.1016/j.bioactmat.2021.04.007>.
- [2] S.F. Spampinato, G.I. Caruso, R. De Pasquale, M.A. Sortino, S. Merlo, The treatment of impaired wound healing in diabetes: looking among old drugs, *Pharmaceuticals* 13 (4) (2020) 60, <https://doi.org/10.3390/ph13040060>.
- [3] G. Frykberg, Robert, Challenges in the treatment of chronic wounds, *Adv. Wound Care* (2015), <https://doi.org/10.1089/wound.2015.0635>.
- [4] Z. Versey, W.S. da Cruz Nizer, E. Russell, S. Zigic, K.G. DeZeeuw, J.E. Marek, J. Overhage, E. Cassol, Biofilm-innate immune interface: contribution to chronic wound formation, *Front. Immunol.* 12 (2021), <https://doi.org/10.3389/fimmu.2021.648554>.
- [5] H. Cho, H.S. Blatchley, E.J. Duh, S. Gerecht, Acellular and cellular approaches to improve diabetic wound healing, *Adv. Drug Deliv. Rev.* 146 (2019) 267–288, <https://doi.org/10.1016/j.addr.2018.07.019>.
- [6] A. Walker, J.A. Brace, Multipurpose dressing: role of a Hydrofiber foam dressing in managing wound exudate, *J. Wound Care* 28 (Sup9a) (2019) S4–S10, <https://doi.org/10.12968/jowc.2019.28.Sup9a.S1>.
- [7] Z. Ma, M. Kotaki, R. Inai, S. Ramakrishna, Potential of nanofiber matrix as tissue-engineering scaffolds, *Tissue Eng.* 11 (1–2) (2015) 101–109, <https://doi.org/10.1089/ten.2005.11.101>.
- [8] D. Hao, H.S. Swindell, L. Ramasubramanian, R. Liu, K.S. Lam, D.L. Farmer, A. Wang, Extracellular matrix mimicking nanofibrous scaffolds modified with mesenchymal stem cell-derived extracellular vesicles for improved vascularization, *Front. Bioeng. Biotechnol.* 8 (2020) 633, <https://doi.org/10.3389/fbioe.2020.00633>.
- [9] A. Memic, T. Abudula, H.S. Mohammed, K. Joshi Navare, T. Colombani, S.A. Bencherif, Latest progress in electrospun nanofibers for wound healing applications, *ACS Applied Bio Materials* 2 (3) (2019) 952–969, <https://doi.org/10.1021/acsbm.8b00637>.
- [10] A. Ghajarieh, S. Habibi, A. Talebian, Biomedical applications of nanofibers, *Russ. J. Appl. Chem.* 94 (7) (2021) 847–872, <https://doi.org/10.1134/S1070427221070016>.
- [11] J. Xue, T. Wu, Y. Dai, Y. Xia, Electrospinning and electrospun nanofibers: methods, materials, and applications, *Chem. Rev.* 119 (8) (2019) 5298–5415, <https://doi.org/10.1021/acs.chemrev.8b00593>.
- [12] D. Sundaramurthi, U.M. Krishnan, S. Sethuraman, Electrospun nanofibers as scaffolds for skin tissue engineering, *Polym. Rev.* 54 (2) (2014) 348–376, <https://doi.org/10.1080/15583724.2014.881374>.
- [13] A. Luraghi, F. Peri, L. Moroni, Electrospinning for Drug Delivery Applications: A Review, *J. Control. Release*, 2021, <https://doi.org/10.1016/j.jconrel.2021.03.033>.
- [14] M.C. Amores de Sousa, C.A. Rodrigues, I.A. Ferreira, M.M. Diogo, R.J. Linhardt, J. Cabral, F.C. Ferreira, Functionalization of electrospun nanofibers and fiber alignment enhance neural stem cell proliferation and neuronal differentiation, *Front. Bioeng. Biotechnol.* 8 (2020) 1215, <https://doi.org/10.1039/D1MA00092F>.
- [15] A. Gomes, C. Teixeira, R. Ferraz, C. Prudêncio, P. Gomes, Wound-healing peptides for treatment of chronic diabetic foot ulcers and other infected skin injuries, *Molecules* 22 (10) (2017) 1743, <https://doi.org/10.3390/molecules22101743>.
- [16] T.N. Demidova-Rice, A. Geevarghese, I.M. Herman, Bioactive peptides derived from vascular endothelial cell extracellular matrices promote microvascular morphogenesis and wound healing in vitro, *Wound Repair Regen.* 19 (1) (2011) 59–70, <https://doi.org/10.1111/j.1524-475X.2010.00642.x>.
- [17] T.N. Lima, C.A. Pedriali Moraes, Bioactive peptides: applications and relevance for cosmeceuticals, *Cosmetics* 5 (1) (2018) 21, <https://doi.org/10.3390/cosmetics5010021>.
- [18] A. Vijayan, C.K. Nanditha, G.V. Kumar, ECM-mimicking nanofibrous scaffold enriched with dual growth factor carrying nanoparticles for diabetic wound healing, *Nanoscale Adv* 3 (11) (2021) 3085–3092, <https://doi.org/10.1039/D0NA00926A>.
- [19] A. Sadeghi-Avalshahr, S. Nokhasteh, A.M. Molavi, M. Khorsand-Ghayeni, M. Mahdavi-Shahri, Synthesis and characterization of collagen/PLGA biodegradable skin scaffold fibers, *Regen. Biomater.* 4 (5) (2017) 309–314, <https://doi.org/10.1093/rb/rbx026>.
- [20] L. Mu, J. Tang, H. Liu, C. Shen, M. Zhang, Z. Rong, R. Lai, A potential wound-healing-promoting peptide from salamander skin, *Faseb. J.* 28 (9) (2014) 3919–3929, <https://doi.org/10.1096/fj.13-248476>.
- [21] C.D. Giornei, T. Sigurdardóttir, A. Schmidtchen, M. Bodelsson, Antimicrobial and chemoattractant activity, lipopolysaccharide neutralization, cytotoxicity, and inhibition by serum of analogs of human cathelicidin LL-37, *Antimicrob. Agents*

- Chemother. 49 (7) (2005) 2845–2850, <https://doi.org/10.1128/AAC.49.7.2845-2850.2005>.
- [22] S. Gera, E. Kankuri, K. Kogermann, Antimicrobial peptides—Unleashing their therapeutic potential using nanotechnology, *Pharmacol. Ther.* (2021) 107990, <https://doi.org/10.1016/j.pharmthera.2021.107990>.
- [23] J.P. Silva, S. Dhall, M. Garcia, A. Chan, C. Costa, M. Gama, M. Martins-Green, Improved burn wound healing by the antimicrobial peptide LLKKK18 released from conjugates with dextrin embedded in a carbopolgel, *Acta Biomater.* 26 (2015) 249–262, <https://doi.org/10.1016/j.actbio.2015.07.043>.
- [24] R. Behrendt, P. White, J. Offer, Advances in Fmoc solid-phase peptide synthesis, *J. Pept. Sci.* 22 (1) (2016) 4–27, <https://doi.org/10.1002/psc.2836>.
- [25] A. Vijayan, P.P. James, C.K. Nanditha, G.V. Kumar, Multiple cargo deliveries of growth factors and antimicrobial peptide using biodegradable nanopolymer as a potential wound healing system, *Int. J. Nanomed.* 14 (2019) 2253, <https://doi.org/10.2147/IJN.S190321>.
- [26] O. Masalova, V. Kulikouskaya, T. Shutava, V. Agabekov, Alginate and chitosan gel nanoparticles for efficient protein entrapment, *Phys. Procedia* 40 (2013) 69–75, <https://doi.org/10.1016/j.phpro.2012.12.010>.
- [27] J.A. Ko, H.J. Park, S.J. Hwang, J.B. Park, J.S. Lee, Preparation and characterization of chitosan microparticles intended for controlled drug delivery, *Int. J. Pharm.* 249 (1–2) (2002) 165–174, [https://doi.org/10.1016/S0378-5173\(02\)00487-8](https://doi.org/10.1016/S0378-5173(02)00487-8).
- [28] J. Jeong, M.J. Conboy, I.M. Conboy, Pharmacological inhibition of myostatin/TGF- $\beta$  receptor/pSmad3 signaling rescues muscle regenerative responses in mouse model of type 1 diabetes, *Acta Pharmacol. Sin.* 34 (8) (2013) 1052–1060, <https://doi.org/10.1038/aps.2013.67>.
- [29] X. Zhang, T. Cui, J. He, H. Wang, R. Cai, P. Popovics, I. Vidaurre, W. Sha, J. Schmid, B. Block, N.L. Ludwig, Beneficial effects of growth hormone-releasing hormone agonists on rat INS-1 cells and on streptozotocin-induced NOD/SCID mice, *Proc. Natl. Acad. Sci. Unit. States Am.* 112 (44) (2015) 13651–13656, <https://doi.org/10.1073/pnas.1518540112>.
- [30] X. Wang, J. Ge, E.E. Tredget, Y. Wu, The mouse excisional wound splinting model, including applications for stem cell transplantation, *Nat. Protoc.* 8 (2) (2013) 302–309, <https://doi.org/10.1038/nprot.2013.002>.
- [31] Y.P. Afsharian, M. Rahimnejad, Bioactive electrospun scaffolds for wound healing applications: a comprehensive review, *Polym. Test.* 93 (2021) 106952, <https://doi.org/10.1016/j.polymertesting.2020.106952>.
- [32] Y. Liang, J. He, B. Guo, Functional hydrogels as wound dressing to enhance wound healing, *ACS Nano* 15 (8) (2021) 12687–12722, <https://doi.org/10.1021/acsnano.1c04206>.
- [33] M. Prabaharan, J.F. Mano, Chitosan-based particles as controlled drug delivery systems, *Drug Deliv.* 12 (1) (2004) 41–57, <https://doi.org/10.1080/10717540590889781>.
- [34] E.M. Tottoli, R. Dorati, I. Genta, E. Chiesa, S. Pisani, B. Conti, Skin wound healing process and new emerging technologies for skin wound care and regeneration, *Pharmaceutics* 12 (8) (2020) 735, <https://doi.org/10.3390/pharmaceutics12080735>.
- [35] M. Takeo, W. Lee, M. Ito, Wound healing and skin regeneration, *Cold Spring Harb. Perspect. Med.* 5 (1) (2015) a023267, <https://doi.org/10.1101/cshperspect.a023267>.
- [36] B. Guo, R. Dong, Y. Liang, M. Li, Haemostatic materials for wound healing applications, *Nat. Rev. Chem.* 5 (11) (2021) 773–791, <https://doi.org/10.1038/s41570-021-00323-z>.
- [37] I. Greco, N. Molchanova, E. Holmedal, H. Jenssen, B.D. Hummel, J.L. Watts, J. Håkansson, P.R. Hansen, J. Svenson, Correlation between hemolytic activity, cytotoxicity and systemic in vivo toxicity of synthetic antimicrobial peptides, *Sci. Rep.* 10 (1) (2020) 1–13, <https://doi.org/10.1038/s41598-020-69995-9>.
- [38] T.M. Honnegowda, P. Kumar, E.G.P. Udupa, S. Kumar, U. Kumar, P. Rao, Role of angiogenesis and angiogenic factors in acute and chronic wound healing, *Plast. Aesthetic Res.* 2 (2015) 243–249, <https://doi.org/10.4103/2347-9264.165438>.
- [39] K.E. Johnson, T.A. Wilgus, Vascular endothelial growth factor and angiogenesis in the regulation of cutaneous wound repair, *Adv. Wound Care* 3 (10) (2014) 647–661, <https://doi.org/10.1089/wound.2013.0517>.
- [40] Y. Liu, Y. Liu, J. Deng, W. Li, X. Nie, Fibroblast growth factor in diabetic foot ulcer: progress and therapeutic prospects, *Front. Endocrinol.* (2021) 1348, <https://doi.org/10.3389/fendo.2021.744868>.
- [41] M. Xue, C.J. Jackson, Extracellular matrix reorganization during wound healing and its impact on abnormal scarring, *Adv. Wound Care* 4 (3) (2015) 119–136, <https://doi.org/10.1089/wound.2013.0485>.
- [42] L.E. Tracy, R.A. Minasian, E.J. Caterson, Extracellular matrix and dermal fibroblast function in the healing wound, *Adv. Wound Care* 5 (3) (2016) 119–136, <https://doi.org/10.1089/wound.2014.0561>.